amygdala to faces that embody either fearful or happy expressions indicates that it may play a similar regulatory role in human social behaviour. □

Methods

Subjects. Four male subjects and one female subject (mean age 42.8 years) took part in the study (approved by the local hospital ethics committee and ARSAC(UK)). All subjects were healthy, with no past history of psychiatric or neurological illness, and were not on any medication. A sixth post-menopausal female subject (age 62 years) was scanned but she was later found to be receiving hormone replacement therapy and was therefore excluded. Inclusion of the data from this subject in the analysis still produced significant activation of the left amygdala ($Z = 3.35$).

PET scan acquisition and analysis. Scans of the distribution of $H_2^{15}O$ were obtained using a Siemens–CPS ECAT EXACT HR$^+$ PET Scanner operated in high sensitivity three-dimensional mode. Subjects received a total of 350 MBq of $H_2^{15}O$ over 20 s through a forearm cannula. Images were reconstructed into 63 planes, using a Hann filter, resulting in a 6.4 mm transaxial and 5.7 mm axial resolution (full-width at half-maximum). The data were analysed with statistical parametric mapping (SPM 95 software, Wellcome Department of Cognitive Neurology, London) implemented in Matlab (Mathworks, Sherborn, MA). After initial realignment, mean PET images from each subject were scalp-edited and used as a template to edit all 12 individual PET images. Structural magnetic-resonance images (MRIs) from each subject were co-registered into the same space. The scans were then transformed into a standard stereotactic space[28]. The scans were smoothed using a gaussian filter set at 12 mm full-width at half-maximum. The rCBF measurements were adjusted to a global mean of 50 ml dl^{-1} min^{-1}. A blocked (by subject) ANCOVA model was fitted to the data at each voxel, with a condition effect for each level of emotional intensity, and global CBF as a confounding covariate. Predetermined contrasts of the condition effects at each voxel were assessed using the usual t-statistic, giving a statistic image for each contrast. The method of SPM data analysis is described in detail in refs 28 and 29.

Experimental design. During each scan, 10 photographs of faces were presented, one at a time, on a computer monitor screen. Each presentation lasted for 3 s, followed by a 2-s interval in which the screen was blank. The 10 faces were of different individuals (5 males and 5 females), but all had the same category and intensity of emotional expression. The faces of the same 10 individuals were used in all 12 scans, in a randomized order. The emotional category and intensity of the faces were varied systematically across scans. The order of presentation of happy and fearful conditions was counterbalanced across subjects. The six different intensity levels were given in a counterbalanced order within and across subjects. In the gender-classification task during scanning, all five subjects identified correctly 90–100% of the time.

Behavioural tests. The validity of the different emotional categories and 'morphed' intensity levels was confirmed using rating and discrimination tests performed on the same subjects, after scanning. In classifying the category (fearful, happy, neutral or 'other'), 96.5% of responses were correct. Subjects then rated the intensity of expression of the face on a 7-point scale. These ratings correlated well with the proportion of the fearful or happy prototype in the morphed face (correlation coefficients: $r = 0.772$ for fearful, $r = 0.826$ for happy). In a separate discrimination test of emotional intensity, different faces were presented in pairs, and subjects selected the more intense expression. Again, there was a close agreement between perceived and 'morphed' intensities: 69.4% of ratings agreed for pairs differing by 25% in their percentage of prototype, 83.3% agreed for pairs differing by 50%, and there was 100% agreement for pairs differing by >50%.

1. Kling, A. S. & Brothers, L. A. in *The Amygdala: Neurobiological Aspects of Emotion, Memory and Mental Dysfunction* (ed. Aggleton, J. P.) 353–377 (Wiley–Liss, New York, 1992).
2. LeDoux, J. E. *Behav. Brain Res.* **58**, 69–79 (1993).
3. Rolls, E. T. in *The Amygdala: Neurobiological Aspects of Emotion, Memory and Mental Dysfunction* (ed. Aggleton, J. P.) 143–167 (Wiley–Liss, New York, 1992).
4. Adolphs, R., Tranel, D., Damasio, H. & Damasio, A. *Nature* **372**, 669–672 (1994).
5. Calder, A. J. *et al. Cogn. Neuropsychol.* **13**, 699–745 (1996).
6. Bechara, A. *et al. Science* **269**, 1115–1118 (1995).
7. LaBar, K. S., LeDoux, J. E., Spencer, D. D. & Phelps, E. A. *J. Neurosci.* **15**, 6846–6855 (1995).
8. Halgren, E., Babb, T. C., Rausch, R. & Crandall, P. H. *Brain* **101**, 83–117 (1978).
9. Darwin, C. *The Expression of the Emotions in Man and Animals* (Univ. Chicago Press, 1965).
10. Ekman, P. *Emotion in the Human Face* (Cambridge Univ. Press, Cambridge, 1982).
11. Ekman, P. & Friesen, W. V. *Pictures of Facial Affect* (Consulting Psychologists, Palo Alto, 1976).
12. Perrett, D. I., May, K. A. & Yoshikawa, S. *Nature* **368**, 239–242 (1994).
13. Halgren, E. in *The Amygdala: Neurobiological Aspects of Emotion, Memory and Mental Dysfunction* (ed. Aggleton, J. P.) 190–228 (Wiley–Liss, New York, 1992).
14. Ketter, T. A. *et al. Arch. Gen. Psychiatry* **53**, 59–69 (1996).
15. Adolphs, R., Tranel, D., Damasio, H. & Damasio, A. *J. Neurosci.* **15**, 5879–5891 (1995).
16. Hamann, S. B. *et al. Nature* **379**, 497 (1996).
17. George, M. S. *et al. J. Neuropsychiatry Clin. Neurosci.* **5**, 384–394 (1993).
18. Sergent, J., Ohta, S., MacDonald, B. & Zuck, E. *Vis. Cogn.* **1**, 349–369 (1994).
19. Herzog, A. G. & Van Hoesen, G. W. *Brain Res.* **115**, 57–69 (1976).
20. Iwai, E. & Yukie, M. *J. Comp. Neurol.* **261**, 362–387 (1987).
21. Aggleton, J. P., Burton, M. J. & Passingham, R. E. *Brain Res.* **190**, 347–368 (1980).
22. Perrett, D. I. *et al. Hum. Neurobiol.* **3**, 197–208 (1984).
23. Perrett, D. I. *et al. J. Exp. Biol.* **146**, 87–114 (1989).
24. Le Doux, J. E., Iwata, J., Cicchetti, P. & Reis, D. J. *J. Neurosci.* **10**, 1062–1069 (1988).
25. Kluver, H. & Bucy, P. C. *Arch. Neurol. Psychiatry* **42**, 979–1000 (1939).
26. Weiskrantz, L. *J. Comp. Phsyiol. Psychol.* **4**, 381–391 (1956).
27. Kling, A. S., Steklis, H. D. & Deutsch, S. *Exp. Neurol.* **66**, 88–96 (1979).
28. Friston, K. J. *et al. Hum. Brain Mapp.* **2**, 189–210 (1995).
29. Friston, K. J. *et al. Hum. Brain Mapp.* **3**, 165–189 (1995).
30. Worsley, K. J. *et al. Hum. Brain Mapp.* (in the press).

Precisely correlated firing in cells of the lateral geniculate nucleus

Jose-Manuel Alonso, W. Martin Usrey* & R. Clay Reid*

Laboratory of Neurobiology, The Rockefeller University, New York, New York 10021, USA

SIMPLE cells within layer IV of the cat primary visual cortex are selective for lines of a specific orientation. It has been proposed that their receptive-field properties are established by the pattern of connections that they receive from the lateral geniculate nucleus (LGN) of the thalamus[1–5]. Thalamic inputs, however, represent only a small proportion of the synapses made onto simple cells[6–8], and others have argued that corticocortical connections are likely to be important in shaping simple-cell response properties[9–11]. Here we describe a mechanism that might be involved in selectively strengthening the effect of thalamic inputs. We show that neighbouring geniculate neurons with overlapping receptive fields of the same type (*on*-centre or *off*-centre) often fire spikes that are synchronized to within 1 millisecond. Moreover, these neurons often project to a common cortical target neuron where synchronous spikes are more effective in evoking a postsynaptic response. We propose that precisely correlated firing within a group of geniculate neurons could serve to reinforce the thalamic input to cortical simple cells.

The projections from the retina to the thalamus are both divergent and convergent. Individual retinal ganglion cells diverge to connect to at least four different geniculate neurons[12]. Conversely, geniculate neurons often receive convergent input from two or more ganglion cells[13]. Although slow correlations have been noted between geniculate neurons[14–16], little attention has been paid to a faster synchrony that may be caused by common input from divergent retinal afferents. Here we have found that extremely fast correlations do exist, and propose a role for them in the transmission of information from thalamus to cortex.

In simultaneous recordings from pairs of closely positioned geniculate cells (electrodes 100–400 μm apart), we occasionally observed firing patterns that were tightly correlated at the 1-ms timescale. These fast correlations were narrower and often stronger than other correlations previously studied in the visual system: between retinal ganglion cells[17–19], between geniculate cells with non-overlapping receptive fields[15,16], between geniculate and cortical cells[3,4] or between cortical cells[20–22].

The strongest fast correlations were between geniculate cells with very similar receptive fields (same position, sign, size and timing). Figure 1a shows the receptive fields of two pairs of *on*-centre geniculate X cells calculated by reverse correlation[23,24]. For

* Present address: Department of Neurobiology, Harvard Medical School, Boston, Massachusetts 02115, USA.

FIG. 1 Two examples of strong, tight correlations between X cells with very similar receptive fields at different delays between stimulus and response. Red, *on* responses. Blue, *off* responses. The brightest colours correspond to the strongest responses. Scale: 0.4 deg per pixel. *a*, Receptive fields. Pair 1–2: two *on*-centre X cells with well overlapped receptive fields of similar size and timing. There is a small difference in the position of the strongest pixels at the centre of the receptive fields. Pair 3–4: two other *on*-centre X cells with almost identical receptive fields. There is only a small difference in the time course of the visual responses; the response in cell 3 is less sustained than in cell 4 (compare the relative strength of the receptive fields at 67 and 86 ms). *b*, Cross-correlations. Pair 1–2: half-width, 0.5 ms; strength, 25%. Pair 3–4: half-width, 1 ms; strength, 43%. The two neurons in each pair were recorded with different electrodes.
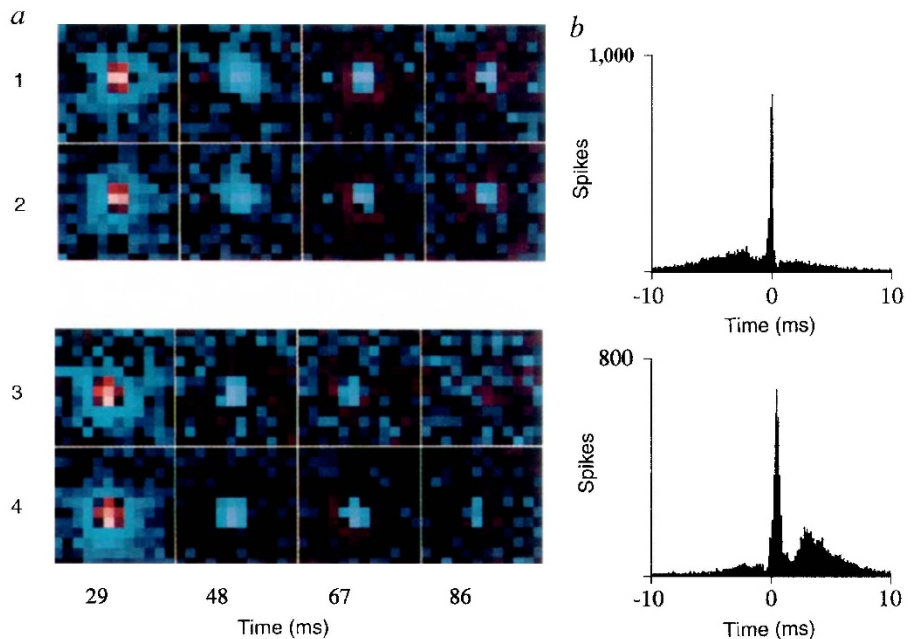
each cell, the time course of the visual response is shown by a series of receptive-field maps calculated for different delays between stimulus and response. The visual responses of each pair of cells (1–2, 3–4) were very similar. When the firing patterns of the cells in each pair were studied by cross-correlation analysis (Fig. 1*b*), we observed very narrow and strong peaks near zero, indicating the neurons often produced spikes within 1 ms of each other (strength of correlation 1–2, 25%; 3–4, 43%).

In addition to the strong correlations seen between cells with nearly identical receptive fields, we occasionally observed weaker correlations between cells with partially overlapped receptive fields. An example of one of these weaker correlations is illustrated in Fig. 2. Shown are the receptive fields of 7 geniculate cells and one synaptic potential, from a retinal input, recorded simultaneously with 5 electrodes. Of the 21 cross-correlations between geniculate cells, only one narrow peak was observed (red circle and inset). This correlation was much weaker (3.3%) than the correlations between cells with nearly identical receptive fields (Fig. 1).

FIG. 2 One example of a weak tight correlation between two X cells with partially overlapped receptive fields (cells E and F). Seven geniculate neurons (A,B,C,E,F,G,H) and a synaptic potential from a retinal input (D) were recorded simultaneously with five different electrodes. The top of the figure shows the 28 possible cross correlations calculated within a time window of 70 ms. E–F (red circle) is the only example of two tightly correlated LGN cells (half-width, 0.5 msec; strength, 3.3%). In the 70 ms correlation, the thin peak is superimposed over the stimulus-dependent correlation. The 10 ms cross-correlation (inset) between cells E and F shows the narrow peak in greater detail. Notice that the strength of this correlation is much weaker than the one shown in Fig. 1. C–D is a correlation between a synaptic potential (D) and an LGN cell (C). The oscillations seen in some of the correlations are stimulus dependent (the white-noise stimulus was updated at 52 Hz). The receptive fields have been smoothed by one half pixel. Black squares correspond to 4 × 4 stimulus pixels, or 1.6°.
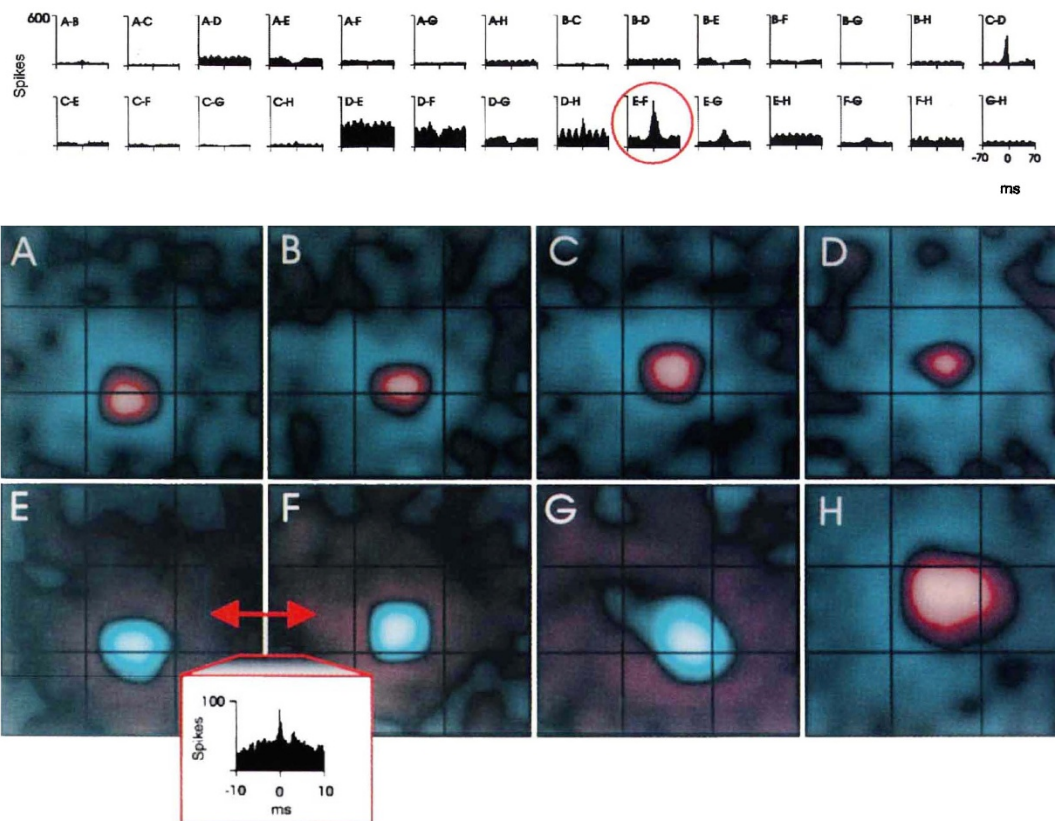
FIG. 3 Two strongly correlated *off*-centre X cells connected to the same simple cell. Receptive fields and cross-correlations: Panels A and B show the receptive fields of two *off*-centre X cells. C is the receptive field of a simple cell. The receptive fields have been smoothed by one half pixel. Black squares correspond to one stimulus pixel, or 0.4°. The two geniculate cells show strong, tightly correlated firing (A–B correlation) which indicates that they probably receive common input from the same ganglion cell (schematically represented by arrows at the top). The cross correlations between the simple cell and each geniculate cell (A → C, B → C) show peaks displaced 2–3 ms to the right of zero which indicate that the simple cell receives monosynaptic input from each geniculate cell[3,4] (schematically represented by arrows on the sides). The red lines are the stimulus-dependent correlations (shuffle correlations[30]). Unlike the intrageniculate correlations, the geniculocortical correlations have a clear presynaptic cell. Geniculocortical correlations, therefore, have been normalized by the number of presynaptic spikes and then expressed in units of spikes per second for the cortical cell. Efficacy of the geniculocortical connection: The spike trains of neurons A and B were divided into two categories: those that occurred within 1.0 ms of each other (A&B) and those of either neuron that did not (A* and B*). The influence of the simultaneous spikes (A&B) was compared to that of the non-simultaneous spikes by adding together the correlograms from A* → C and B* → C (middle panels). Efficacy was calculated as the percentage of thalamic spikes followed by a cortical spike after subtracting the shuffle correlation[3,4]. The summed efficacy of the non-simultaneous spikes (A* and B*) was 3.12 ± 0.30% (efficacy of A* = 1.71 ± 0.07%; efficacy of B* = 1.41 ± 0.22%) whereas that of the simultaneous spikes (A&B) was 5.28 ± 0.23%. Each of these values may be slight underestimates of the actual efficacies. This is because the baseline subtraction, or shuffle correction, itself includes a contribution from the geniculate neuron under study. This potential source of error, however, is relatively small compared with the 69% difference in calculated efficacies. As these neurons were studied over a long period, there were sufficient spikes in all categories to study their influence on C (A: 64,779; B: 16,784; A*: 58,054; B*: 10,059; A&B: 13,450; C: 8,635).
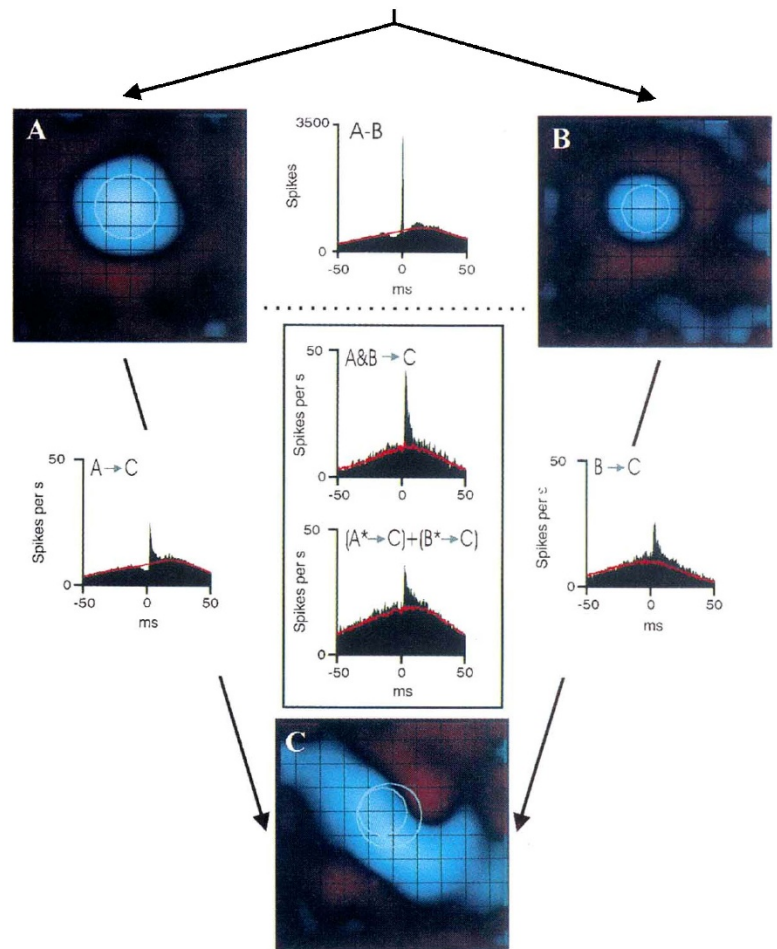
We recorded from 282 pairs of geniculate cells with some degree of overlap between their receptive field centres or surrounds (Table 1). All of the cell pairs with nearly identical receptive fields were correlated on the ms timescale; further, these correlations were very strong (average, 28%). Receptive fields that differed in any respect (position, size, sign or timing) were less likely to be correlated and the correlations were much weaker.

Several lines of evidence suggest that the strong, tight correlations shown in Fig. 1 are the result of inputs from a common retinal ganglion cell. Strong correlations were seen only between geniculate cells with very similar receptive fields (Table 1). Additionally, in two experiments we observed a common synaptic potential or a T-waveform (spike from the retinal axon) preceding the spikes of both correlated cells. The rather low percentage of tightly correlated cells (15%) fits well with the anatomical data, which indicates that only 10% of neighbouring geniculate cells receive input from any given ganglion cell[12].

The precisely correlated firing of geniculate neurons could be important for the development of the thalamocortical projection[25] or may provide the substrate for neuronal coding strategies based on precise timing[19,26]. A related possibility is that synchronous inputs from several thalamic cells could interact to increase their effectiveness in driving a common cortical target.

To test the hypothesis that simultaneous thalamic spikes are more effective than non-simultaneous spikes, we examined the interactions between several geniculate cells connected to a common simple cell. Figure 3 shows an example of two precisely correlated, off-centre X cells (A, B in Fig. 3) connected to the same simple cell (C). The correlogram at the top of the figure (A–B) shows a strong, fast correlation between the two X cells (as in Fig. 1). The geniculocortical correlations (A → C, B → C) indi-

cate that the X cells were monosynaptically connected to the simple cell[3,4].

We examined a potential role for the simultaneous firing of the two thalamic neurons by dividing their spikes into two categories: those that occurred within 1.0 ms of each other (A&B) and those of either neuron that did not (A* and B*). If the separate influences from thalamic neurons A and B on the cortical cell were added together independently, then the peak in the summed correlogram from the non-simultaneous spikes (Fig. 3; (A* → C) + (B* → C)) should resemble the peak in the correlogram for the simultaneous spikes (A&B → C). Instead, the size of the peak (above the stimulus-dependent portion, red line) was much greater for the simultaneous spikes. As calculated from these correlograms, the efficacy of simultaneous spikes (A&B, efficacy 5.28 ± 0.23%) was larger than the summed efficacy of non-simultaneous spikes (A* and B*, summed efficacy 3.12 ± 0.30).

We studied thirteen cases where two geniculate cells were connected to a common simple cell. In each case, simultaneous thalamic spikes (A&B) were more effective in driving the cortical neuron than non-simultaneous spikes (A* or B*) from either neuron. Further, in 11 of 13 cases, the efficacies of simultaneous spikes (A&B) were greater than the sum of the efficacies of A* + B* (mean 71%, median 50%; P < 0.01, paired student *t*-test). Included in the 11 cases were two pairs of geniculate cells with completely overlapped receptive fields that showed precisely correlated firing. The remaining 9 cases were from geniculate cell pairs in which both cells were connected to a common cortical neuron, but were not themselves correlated. These cases serve as an important control, as discussed below.

Two possible mechanisms that might be responsible for the

Overlap of RF centres	Per cent positively correlated	Strength of positive correlations*
No overlap	0% (0/73)	–
	XX: 0/43; XY: 0/28; YY: 0/2	
Partial overlap	17% (28/167)	1.9% (n = 20)
	XX: 17/101; XY: 7/51; YY: 4/15	XX: 12; XY: 5; YY: 3
Total overlap	48% (20/42)	10% (n = 12)
	XX: 14/18; XY: 6/23; YY: 0/1	XX: 8; XY: 4
and same sign	52% (14/27)	13% (n = 9)
	XX: 10/12; XY: 4/14 YY: 0/1	XX: 6; XY: 3
and similar size	79% (10/13)	23% (n = 5)
	XX: 10/12; YY: 0/1	XX: 5
and similar timing	100% (6/6)	28% (n = 4)
	XX: 6/6	XX: 4

Percentage of positively correlated geniculate cells and correlation strengths as a function of receptive field overlap. Cell pairs with nearly identical receptive fields were more frequently correlated and the correlations were very strong. Receptive fields that differed in any respect (position, size, sign or timing) were less likely to be correlated and the correlations were much weaker. Total overlap: when the centres of the two receptive fields were completely superimposed or when one was contained in the other. No overlap: when the centres of the receptive fields shared no common pixels. Partial overlap: all other cases. Similar size: when the difference in the diameter of the two receptive field centres was less than or equal to 0.8° (two pixels). Similar timing: when $|a_0 - a_1| + |b_0 - b_1| + |c_0 - c_1| + |d_0 - d_1|$ was less than three units, where for a given on-centre cell a is the time of the first frame that contains a significant on-response (20% larger than noise), b is the time of the frame with the strongest on-response, c is the time of the first frame with significant off-rebound and d is the time of the frame with the strongest off-rebound. Note that the sample size in columns 'correlation' and 'strength' is different because only cell pairs recorded with different electrodes were used for determining the strength of correlations. Fast correlations were observed with white-noise, drifting gratings and in the absence of visual stimuli.

* Strength of correlations calculated only for LGN cells recorded with different electrodes.

increased efficacy of simultaneous spikes are that simultaneous excitatory postsynaptic potentials are more likely to bring the neuron to threshold[27], or that they engage some other nonlinear biophysical mechanism in the soma or dendrites (such as calcium action potentials[28]). Our study cannot distinguish between these possibilities. An alternative explanation is that other strongly correlated geniculate inputs (not recorded) might be responsible for the observed larger efficacy of simultaneous spikes.

Our results indicate, however, that other strongly correlated inputs alone cannot explain the increased efficacy of simultaneous spikes. Non-correlated pairs of geniculate cells also produce simultaneous spikes (A&B), but these events occur infrequently and randomly. There is little chance, therefore, that these random simultaneous spikes are strongly correlated with the spikes of other geniculate neurons. However, in 9 of 11 cases, random simultaneous spikes were more effective in driving a simple cell. One such example is shown in Fig. 4. A pair of non-overlapping X and Y geniculate cells of opposite sign (cells A and B) were recorded from simultaneously, along with an appropriately overlapped simple cell (C). As expected, the geniculate cells were not tightly correlated in their firing. Nevertheless, the efficacy of the simultaneous spikes (A&B, efficacy $5.51 \pm 0.32\%$) was larger than the summed efficacy of the non-simultaneous spikes (A* and B*, summed efficacy $3.60 \pm 0.22\%$). As emphasized by the control shown in Fig. 4, nearly simultaneous spikes do occur by chance. However, the overall frequency of synchronized spikes is increased by the systematic correlations reported here.

It must be noted that whereas synchrony may increase the influence of thalamic neurons on their postsynaptic target, it may lead to overestimates of efficacy in cases where only a single geniculate and cortical cell are studied[3,4]. Given the size

FIG. 4 Two uncorrelated geniculate cells (on-centre X, off-centre Y) connected to the same simple cell. The receptive fields have been smoothed by one half pixel. Black squares correspond to one stimulus pixel, or 0.4°. Panels A and B show the receptive fields of an on-centre X cell and an off-centre Y cell. These two geniculate cells do not show strong, tightly correlated firing (A–B correlation). Therefore, this example serves as a control to demonstrate that the increased efficacy seen in Fig. 3 is not merely due to the existence of a small ensemble of strongly correlated cells. C is the receptive field of a cortical simple cell. The geniculocortical correlations (A → C, B → C) indicate that each geniculate cell is monosynaptically connected to the simple cell[3,4]. The red lines are the stimulus-dependent correlations (shuffle correlations[30]). Efficacy of A* = 0.46 ± 0.08; efficacy of B* = $3.14 \pm 0.13\%$; efficacy of A* + efficacy of B* = $3.60 \pm 0.22\%$; efficacy of A&B = $5.51 \pm 0.32\%$. Number of spikes collected (A: 166,151; B: 54,114; A*: 162,330; B*: 50,300; A&B: 7,635; C: 51,138.
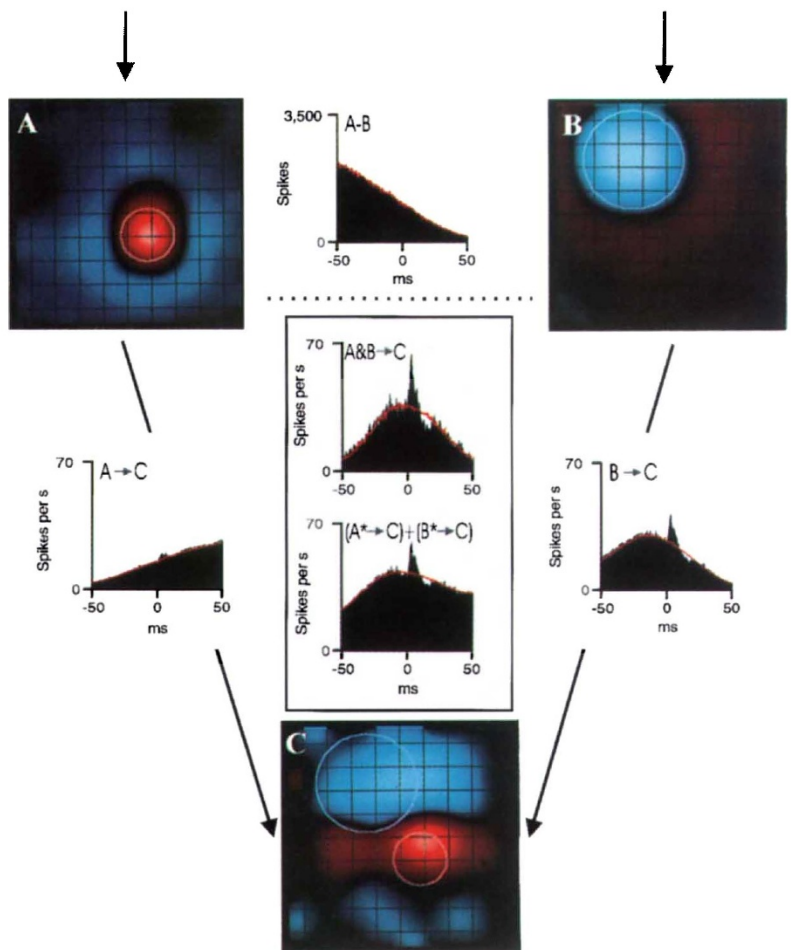
and frequency of intrageniculate correlations (Table 1), however, this overestimate should not be very large. Fast intrageniculate correlations could also lead to qualitative errors. A positive thalamocortical correlation could be found when a geniculate cell was not in fact connected to a particular cortical neuron but instead was highly correlated with another geniculate cell that was connected to the cortical neuron. Such 'false positives' would not strongly affect previous conclusions about the specificity of geniculocortical connections[4], because strong intrageniculate correlations are seen only between cells with nearly identical receptive fields. It is thus also unlikely that nonlinear interactions between synchronous inputs (Fig. 3) have a direct effect on receptive field properties, such as orientation selectivity.

To summarize, precisely correlated firing could serve to strengthen the thalamic input to cortical cells[3,4]. This form of strengthening would act in addition to other factors, including: the size and position of geniculate boutons on the postsynaptic cell[8], active dendritic conductances[29], the high firing rate of geniculate afferents, and the slower correlations within the retina and thalamus[14-19]. Moreover, intracortical excitation must also play a role in determining the sensitivity of cortical cells to geniculate input[9-11]. On the basis of the findings reported here, the divergence from a single ganglion cell to several cells in the LGN would converge again onto an individual cortical simple cell. This reconvergence would secure the transmission of information[26] from retina to visual cortex. □

Methods

Recordings were made from anaesthetized and paralysed cats[4]. Nearby geniculate cells were recorded with a single electrode (42 pairs; 16 pairs correlated), and with different electrodes[29] (240 pairs; 32 pairs correlated). Spike isolation was based on cluster analysis of waveforms (Datawave Systems, Broomfield, Colorado) and presence of a refractory period (shape of autocorrelations). To test the significance level of the tight correlations between geniculate cells, cross correlations were bandpass filtered between 75 and 700 Hz. The significance level was set at a probability of 1.2%, assuming a normal distribution in the baseline amplitudes after filtering. The strength of the correlation was obtained from the unfiltered correlograms[4].

1. Hubel, D. H. & Wiesel, T. N. J. Physiol. (Lond.) 160, 106–154 (1962).
2. Chapman, B., Zahs, K. R. & Stryker, M. P. J. Neurosci. 11, 1347–1358 (1991).
3. Tanaka, K. J. Neurophysiol. 49, 1303–1318 (1983).
4. Reid, R. C. & Alonso, J. M. Nature 378, 281–284 (1995).
5. Ferster, D., Chung, S. & Wheat, H. Nature 380, 249–252 (1996).
6. LeVay, S. & Gilbert, C. D. Brain Res. 113, 1–19 (1976).
7. Peters, A. & Payne, B. R. Cerebral Cortex 3, 69–78 (1993).
8. Ahmed, B., Anderson, J. C., Douglas, R. J., Martin, K. A. C. & Nelson, J. C. J. Comp. Neurol. 341, 39–49 (1994).
9. Douglas, R. J., Koch, C., Mahowald, M., Martin, K. A. & Suarez, H. H. Science 269, 981–985 (1995).
10. Somers, D. C., Nelson, S. B. & Sur, M. J. Neurosci. 15, 5448–5465 (1995).
11. Stratford, K. J., Tarczy-Hornoch, K., Martin, K. A. C., Bannister, N. J. & Jack, J. J. B. Nature 382, 258–261 (1996).
12. Hamos, J. E., Van Horn, S. C., Raczkowski, D. & Sherman, S. M. J. Comp. Neurol. 259, 165–192 (1987).
13. Cleland, B. G., Dubin, M. W. & Levick, W. R. Nature New. Biol. 231, 191–192 (1971).
14. Stevens, J. K. & Gerstein, G. L. J. Neurophysiol. 39, 239–256 (1976).
15. Sillito, A. M., Jones, H. E., Gerstein, G. L. & West, D. C. Nature 369, 479–482 (1994).
16. Neuenschwander, S. & Singer, W. Nature 379, 728–732 (1996).
17. Rodieck, R. W. J. Neurophysiol. 30, 1043–1071 (1967).
18. Mastronarde, D. N. Trends Neurosci. 12, 75–80 (1989).
19. Meister, M., Lagnado, L. & Baylor, D. A. Science 270, 1207–1210 (1995).
20. Toyama, K., Kimura, M. & Tanaka, K. J. Neurophysiol. 46, 191–201 (1981).
21. Ts'o, D. Y., Gilbert, C. D. & Wiesel, T. N. J. Neurosci. 6, 1160–1170 (1986).
22. Singer, W. & Gray, C. M. Annu. Rev. Neurosci. 18, 555–586 (1995).
23. Jones, J. P. & Palmer, L. A. J. Neurophysiol. 58, 1233–1258 (1987).
24. Sutter, E. Adv. Meth. Physiol. Systems Model 1, 303–315 (Univ. Southern California, 1987).
25. Meister, M., Wong, R. O. L., Baylor, D. A. & Shatz, C. J. Science 252, 939–943 (1991).
26. Dan, Y., Alonso, J. M., Usrey, W. M. & Reid, R. C. Soc. Neurosci. Abstr. 22, 1703 (1996).
27. Jagadeesh, B., Wheat, H. S. & Ferster, D. Science 262, 1901–1904 (1993).
28. Hirsch, J. A., Alonso, J. M. & Reid, R. C. Nature 378, 612–616 (1995).
29. Eckhorn, R. & Thomas, U. J. Neurosci. Methods. 49, 175–179 (1993).
30. Perkel, D. H., Gerstein, G. L. & Moore, G. P. Biophys. J. 7, 419–440 (1967).

Loss of morphine-induced analgesia, reward effect and withdrawal symptoms in mice lacking the μ-opioid-receptor gene

Hans W. D. Matthes*, Rafael Maldonado†,
Frédéric Simonin*, Olga Valverde†, Susan Slowe‡,
Ian Kitchen‡, Katia Befort*, Andrée Dierich§,
Marianne Le Meur§, Pascal Dollé§, Eleni Tzavara∥,
Jacques Hanoune∥, Bernard P. Roques†
& Brigitte L. Kieffer*

* UPR 9050 CNRS, ESBS Université Louis Pasteur, 67400 Illkirch, Strasbourg, France
† Département de Pharmacochimie Moléculaire et Structurale, INSERM U266. URA D1500 CNRS, Université René Descartes, 75270 Paris, France
‡ Receptors and Cellular Regulation Research Group, School of Biological Sciences, University of Surrey, Guildford, Surrey GU2 5XH, UK
§ Institut de Génétique et Biologie Moléculaire et Cellulaire, BP 163, 67404 Illkirch, Strasbourg, France
∥ Unité de Recherches INSERM U-99, Hôpital Henri Mondor, 94010 Créteil, France

DESPITE tremendous efforts in the search for safe, efficacious and non-addictive opioids for pain treatment, morphine remains the most valuable painkiller in contemporary medicine. Opioids exert their pharmacological actions through three opioid-receptor classes[1,2], μ, δ and κ, whose genes have been cloned[3]. Genetic approaches are now available to delineate the contribution of each receptor in opioid function in vivo. Here we disrupt the μ-opioid-receptor gene in mice by homologous recombination and find that there are no overt behavioural abnormalities or major compensatory changes within the opioid system in these animals. Investigation of the behavioural effects of morphine reveals that a lack of μ receptors abolishes the analgesic effect of morphine, as well as place-preference activity and physical dependence. We observed no behavioural responses related to δ- or κ-receptor activation with morphine, although these receptors are present and bind opioid ligands. We conclude that the μ-opioid-receptor gene product is the molecular target of morphine in vivo and that it is a mandatory component of the opioid system for morphine action.

The μ-opioid-receptor (MOR) gene was inactivated in P1 embryonic stem (ES) cells from the 129/Sv mouse line by insertion of a neomycin-resistance (neo^r) cassette in the gene coding region (Fig. 1a). Gene targeting was identified by Southern blotting using a 5′ probe (Fig. 1b), giving 7 positives out of 90 neomycin-resistant clones analysed. Further Southern analysis using a 3′ probe and the neo^r probe confirmed accurate integration of a single copy of the disrupted MOR gene fragment (not shown). One positive ES clone was used to establish mutant mice (Fig. 1c).

Mice genotyping showed that heterozygous offspring followed the expected mendelian frequency, with 28.6% wild-type, 46.6% heterozygous and 24.8% homozygous animals (n = 178), indicating that there was no in utero or postnatal mortality of mutant MOR mice. No obvious morphological abnormalities could be detected in homozygous mutant mice. MOR-deficient mice did not differ from their littermates in health or growth. Homozygous mice were fertile and bred normally, with no impairment of maternal behaviour.